Support Vector Regression Based Multivariate Lesion-Symptom Mapping

Yongsheng Zhang, Daniel Y. Kimberg, H. Branch Coslett, Myrna F. Schwartz, Ze Wang, *IEEE Member*

***Abstract*—A novel multivariate lesion-symptom mapping (LSM) methodology was developed in this study. Lesion analysis is a classic model for studying brain functions. Using lesion data, focal brain-behavior associations have been widely assessed using the massive voxel-based lesion symptom mapping (VLSM) method. Assessing each voxel independently, VLSM suffers from low sensitivity after correcting for the enormous number of comparisons. It is also incapable for assessing a spatially distributed association pattern though the brain-behavior associations generally involve a collection of functionally related voxels. To solve these two outstanding problems, we carried out the first multivariate lesion symptom mapping (MLSM) in this study using support vector regression (SVR). In the so dubbed SVR-LSM, the symptom relation to the entire lesion map rather than each isolated voxel is modeled using a non-linear function, so the inter-voxel correlations are intrinsically considered, resulting in a potentially more sensitive way to examine lesion-symptom relationships. Evaluations using synthetic data and real data showed that SVR-LSM gained a much better performance (in terms of sensitivity and specificity) for detecting brain-behavior relations than VLSM. While the method was designed for lesion analysis, extending it to neuroimaging data will be straightforward.**

I. Introduction

Localizing brain-behavior relationships is a major goal of cognitive neuroscience and clinical neurology. Structural imaging based lesion-symptom mapping (LSM) has long been used to study brain-behavior relationships [1] and complements what can be learned from functional neuroimaging by providing high-quality evidence that the integrity of a brain region is necessary for the normal performance of the measured function [2]. VLSM [1] has been a standard statistical LSM method for assessing brain-behavior relationships. In VLSM, behavioral measurement difference between patients with and without lesion is assessed on a voxel-by-voxel basis. The significance of the behavioral difference associated with lesion status is used to indicate the importance of brain regions for the considered function. But the univariate feature of VLSM makes it suboptimal for assessing the multivariate lesion-symptom relationship [3].

While multivariate method has been increasingly used in neuroimaging, an MSLM is still lacking. In a preliminary study [4], we piloted partial least square (PLS) as an MLSM. However, it requires entering several behavioral scores into the same PLS model, and degrades to VLSM when only one behavior score is included.

Support vector machine (SVM) and logistic regression have been introduced to predict the presence of some symptoms in [5] and [6], respectively. But these methods rest on dichotomized behavioral classification, a drawback in cases where performance grades continuously between two diagnoses, or between pathology and normality. In [7], we piloted a machine learning regression, the support vector regression (SVR) [8], to predict language dysfunction using the spatial geometrical features of lesions.

The purpose of this study was to develop and evaluate a SVR-based MLSM. SVR is an extension of support vector machine (SVM) [9], which has been used in many brain imaging studies [10] and lesion analysis as well [5]. While an SVM model is trained to optimally separate the input data by categories, an SVR model is trained to best predict a continuous association variable (the behavioral measure in LSM) using all independent variables (here, all voxels' lesion statuses) [8,11]. This multivariate input-output relationship mapping fits precisely the goals of MLSM. By introducing SVR into LSM, we hypothesized that brain-behavior association detection sensitivity of LSM will be greatly improved.

The paper is organized as: method, evaluations with previously published lesion data [12] and both synthetic and real behavior scores, results and discussion.

II. The Proposed SVR-LSM Method

Suppose the lesion maps are $\boldsymbol{X} = (\boldsymbol{x_0}, \boldsymbol{x_1}, \boldsymbol{x_2}, \cdots, \boldsymbol{x_{M-1}})$, each element representing a lesion map with N voxels: $\boldsymbol{x_m} = (x_m^0, x_m^1, x_m^2, \cdots, x_m^{N-1})^T$, $(m = 0, \ldots, M-1$, M is the number of subjects), and the behavior score is $\boldsymbol{y} = (y_0, y_1, y_2, \cdots, y_{M-1})^T$. LSM can be equivalently expressed as a multiple regression model:

$$\boldsymbol{y} = \boldsymbol{X}^T\boldsymbol{\beta} + \boldsymbol{b} \tag{1}$$

where, $\boldsymbol{\beta} = (\beta_0, \beta_1, \beta_2, \cdots \beta_{N-1})^T$ are the fitting coefficients with β_j representing the lesion-behavior association strength at the j-th voxel x_j, and $\boldsymbol{b} = (b_0, b_1, b_2, \cdots b_{M-1})^T$ are the fitting errors.

Because there are usually much more unknown variables than observations (N>>M, N can be up to millions), the inverse problem of (1) is generally ill-positioned. Additional information is then required to select a practically meaningful and interpretable solution out of the many.

A. Support Vector Regression (SVR)

SVR solves the above mentioned under-determined problem by requiring the regression model to be "flat" or

This work was supported by the National Institute on Deafness and Other Communication Disorders (NIDCD) at National Institutes of Health (NIH) (R21DC011074 and R01DC000191).

Y. Zhang and Z. Wang are with the University of Pennsylvania, Philadelphia, PA 19104, USA (correspondence to: Ze Wang; phone: 215-222-3200 ext 123; email: zewang@mail.med.upenn.edu)

smooth to allow the model to be less fitted to the training data but more flexible for predicting new data. "Flatness" here is measured by the norm of fitting coefficients.

For the i-th subject's lesion map $\boldsymbol{x_i}$ and behavior score y_i, the SVR model can be described by

$$y_i = \boldsymbol{w}^T \phi(\boldsymbol{x}_i) + b \tag{2}$$

where $\phi(\boldsymbol{x}_i)$ is the function transforming the independent variable (lesion data in this paper) to a higher (even infinite) dimensional feature space, $\boldsymbol{w} = (w_0, w_1, w_2, \cdots)^T$ is the fitting coefficient in the high dimensional space, and b is the fitting error. Except for the transform, this model is the same as that described in (1); and both operate in a map-wise manner, in contrast with the voxel-wise approach used in standard VLSM.

With the "flatness" constraint, (2) can be expressed as a Lagrangian multiplier-based minimization problem [11]:

$$\text{min: } E(\boldsymbol{w}) = \frac{1}{2}\|\boldsymbol{w}\|^2 + C\sum_{i=0}^{M-1}(\xi_i - \xi_i^*) \tag{3}$$

$$\text{s.t.: } \begin{cases} y_i - \langle w, \phi(x_i)\rangle - b \le \epsilon + \xi_i \\ \langle w, \phi(x_i)\rangle + b - y_i \le \epsilon + \xi_i^* \\ \xi_i, \xi_i^* \ge 0 \end{cases}$$

where, constant C controls the tradeoff between the flatness $\|\boldsymbol{w}\|^2$ and the tolerable fitting error [8], ξ_i and ξ_i^* are slack variables to cope with losses outside of the soft margins. $|\xi|_\epsilon$ is a ϵ-insensitive error function, it equals to 0 if $|\xi| < \epsilon$, otherwise it equals to $|\xi| - \epsilon$ [8].

Equation (3) is usually solved in its dual form:

$$\begin{aligned} L :=& \frac{1}{2}||w||^2 + C\sum_{i=0}^{M-1}(\xi_i + \xi_i^*) - \sum_{i=0}^{M-1}(\eta_i\xi_i + \eta_i^*\xi_i^*) \\ &- \sum_{i=0}^{M-1}\alpha_i(\epsilon + \xi_i - y_i + < w, \phi(x_i) > + b) \\ &- \sum_{i=0}^{M-1}\alpha_i^*(\epsilon + \xi_i^* + y_i - < w, \phi(x_i) > - b) \end{aligned} \tag{4}$$

where, L is the Lagrangian, η_i, η_i^*, α_i and α_i^* are Lagrange multipliers no less than 0. Solving the Lagrangian equation in (4), and with the help of *kernel trick*, $k(x_i, x_j) = \langle\phi(x_i), \phi(x_j)\rangle$, the multiple regression model in (2) could be written as

$$f(x) = \sum_{i=0}^{M-1}(\alpha_i - \alpha_i^*)\langle\phi(x_i), \phi(x)\rangle + b, \tag{5}$$

where, $(\alpha_i - \alpha_i^*)$ is simplified as λ_i without introducing any ambiguity [13], and was in the following of this paper. Please refer to [9] and [11] for detailed description about SVR algorithm.

B. SVR-LSM

In order to identify lesion-behavior association in a brain anatomical sense, the nonlinear lesion-behavior association captured by SVR needs to be projected back to the original input data space. This can be done by a "pre-image" process or a "sensitivity mapping". Pre-image is to find a direct inverse transform of the SVR kernel, which is usually non-trivial. Sensitivity mapping characterizes sensitivity of the model output (behavior scores) to each input data (lesion map) dimension by calculating partial derivative of the output variable to the original input variable and then taking the sum over all input data. It has been used in several studies for visualizing a nonlinear classifier [14] and was used in this paper. For SVR-LSM, sensitivity of each voxel reflects the relative contributing weight of each voxel in the original image space to the SVR hyperplane for predicting the model output (behavior scores). Higher sensitivity means the voxel is more associated with the assessed behavior measurement.

Following Rasmussen et al.'s work [14], sensitivity of a given behavior score $\boldsymbol{y}$ with respect to voxel lesion status x_j can be empirically calculated as

$$\hat{s}_j = \frac{1}{M}\sum_{i=1}^{M}\left(\frac{\partial\lambda^T\boldsymbol{k_x}}{\partial x^j}\right)_{\boldsymbol{x}=\boldsymbol{x}_i} \tag{6}$$

Where, $\boldsymbol{k_x}$ is an M dimensional column vector with elements $\boldsymbol{k}_{\boldsymbol{x}}^{(i)} = k(\boldsymbol{x}_i, \boldsymbol{x})$, x_i is the lesion status of the i-th voxel. For the RBF kernel, $\boldsymbol{k}_{\boldsymbol{x}}^{(i)} = \exp\left(-\frac{\|\boldsymbol{x_i}-\boldsymbol{x}\|^2}{\gamma}\right)$, its derivative is

$$\frac{\partial\lambda^T\boldsymbol{k_x}}{\partial x^j} = \sum_i \lambda_i 2\frac{x_i^j - x^j}{\gamma}\exp\left(-\frac{\|\boldsymbol{x_i}-\boldsymbol{x}\|^2}{\gamma}\right). \tag{7}$$

The sign cancellation problem of (7) [14] is less problematic for lesion data because there are large amount of subjects don't have lesion at many voxels, so they won't contribute to the summation process. Additionally those subjects showing large distance from the evaluated one ($\|\mathrm{x_i} - \mathrm{x}\|^2$) will have very minor contribution because the exponential term becomes close to 0. A quadratic formula can still be used if there is severe sign cancellation.

III. Evaluations using Synthetic and Real Data

Patients with aphasia caused by left hemisphere stroke were recruited from the Neuro-Cognitive Rehabilitation Research Patient Registry at the Moss Rehabilitation Research Institute [15] or the Centre for Cognitive Neuroscience Patient Database at the University of Pennsylvania. Structural MRI (n=60) or CT (n=46) brain imaging was done under a protocol approved by the IRB at the University of Pennsylvania Medical School to obtain precise anatomical data. Lesions were manually segmented on the structural image by a trained technician or experienced neurologist, both of whom were blinded to the behavioral data (please refer to details in [12]).

The PNT (Philadelphia Naming Test [16]) basic-level object naming capability with 175 object depictions from a variety of semantic categories. Semantic errors (SE) represent failure to select the right word based on its meaning; they are real words that bear a semantic relation to the target. In analysis for both synthetic and real scores, only voxels lesioned in ≥ 10 patients were included.

A. Synthetic score

Synthetic lesion-behavior relations were inserted into 3 *a priori* cubic ROIs (shown in Fig. 1a) based on the actual lesion data from the 106 subjects. Each ROI was a $21 \times 21 \times 21mm^3$ cube. The synthetic score was generated as the mean lesion volume ratio of these three ROIs, and normalized to range [0, 100].

The ROIs were positioned at different locations to represent different correlations between the local lesion status and the total lesion volume. For example, the lesion status of voxel within ROI-3 is much less correlated to the total lesion

volume (with mean correlation coefficient (CC) of 0.2942) than voxels within ROI-1 and ROI-2 (with mean CC of 0.7301 and 0.7002, respectively), as shown in Fig. 1b. Usually, larger total lesion volume leads to more severe behavior dysfunction, it is a typical confound preventing localizing the specific regions for the considering function. As for the synthetic score, a superior LSM method should successfully localize all the three association regions, while an inferior LSM method may fail to localize ROI-3 because its correlation to the total lesion volume is low.

B. SVR-LSM

For each subject, the lesion statuses of all voxels in the valid voxel mask were grouped into one column vector. As a general preprocessing step in SVR, each subject's lesion data vector was normalized to have a unit norm, i.e., the square root of the sum of squared elements for each vector equal to 1. The normalized vectors from all participants were combined into a feature matrix with rows representing different subjects. The language scores were also input into a column vector and normalized. An ϵ-SVR model with RBF kernel was used to estimate the SVR hyperplane. In this work, libSVM [17] was used for implementing SVR.

To find the optimal values for parameter C and γ, both of them were changed from 2^{-2} to 2^{7} with a growth ratio of 2. At each particular C and γ, SVR-LSM was used to identify the synthetic brain-behavior relations. The receiver operator characteristic (ROC) [18] was calculated and the area under the ROC curves (AUC) was collected as the objective function. The optimum point was found to locate at $(C = 32, \gamma = 1)$ where AUC reached maximum. This set of values was then used in all the following experiments. 40 times 5-fold cross-validations were then performed to assess the prediction accuracy of SVR-LSM. Each validation used a randomly selected lesion and behavior data from 4/5 of the entire patients to train the SVR model, and the rest 1/5 subjects for testing.

C. Simple regression-based VLSM

VLSM analysis was performed by running a voxel-wise simple regression analysis, with the lesion status as the independent variable and the behavior score as the dependent variable. To give a fair comparison, the lesion data vector for each subject was also normalized to have a unit norm. The fitting coefficient map (beta-map) was converted into a t-map using SPM (www.fil.ion.ucl.ac.uk/spm/, Wellcome Institute of Imaging Neuroscience, London, UK).

D. Statistical inference for LSM maps

To provide a statistical inference, 1000 permutations were performed by randomly permuting the behavior score. For each permutation, LSM parameter maps (t-map for VLSM and sensitivity map for SVR-LSM) were collected and compared to those obtained from the genuine data, and the number of permutations yielding higher value than the genuine one was divided by 1001 to get the permutation p-value.

IV. Results and Discussion

A. Synthetic lesion-behavior relation detection

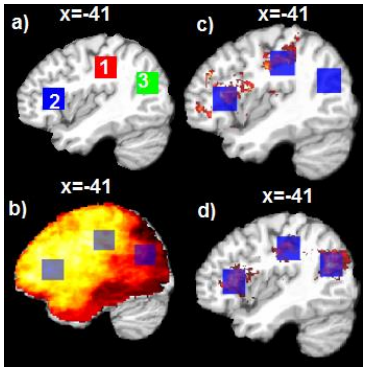

Fig. 1. Predefined ROIs and LSM results for the lesion-synthetic score association. a) Predefined ROIs for generating synthetic score; b) The correlation map between the lesion status of each voxel and the total lesion volume. c) Thresholded VLSM t-map; d) Thresholded SVR-LSM sensitivity map.

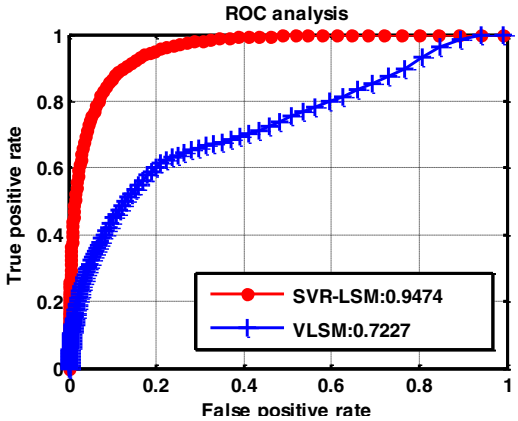

Fig. 2. ROC curves of SVR-LSM and VLSM method for the lesion-synthetic score relationship. The AUC values for different methods are shown in the legend.

Fig. 1c and 1d show the results of VLSM and SVR-LSM for localizing the synthetic lesion-behavior associations. The parametric maps of VLSM and SVR-LSM were thresholded separately to make the number of suprathreshold voxels equals to the total volume of these 3 ROIs, in order to directly compare both the true positive and false positive voxels. As shown in Fig 1, SVR-LSM showed much higher sensitivity in ROI 1 and 3 (Fig. 1d), while VLSM could not detect ROI 3 (Fig. 1c).

Fig. 2 shows the ROC curves of VLSM and SVR-LSM for the same synthetic data used above. To calculate the ROC curves, LSM results were thresholded with descending threshold. At each threshold, a true positive rate (proportion of suprathreshold voxels within the ROIs) and a false positive rate (proportion of suprathreshold voxels outside the ROIs) were calculated. A better performing LSM method should yield a ROC curve that is closer to the true positive axis while farther away from the false positive axis. The area under the curve (AUC) was calculated to quantify the performance, where a larger AUC means better performance. Consistent with results shown in Fig. 1c and 1d, SVR-LSM yielded significantly higher ROC performance than VLSM as indicated by the AUC value.

B. Detection of the lesion-SE relations

Fig. 3a and 3b show the non-thresholded VLSM t-map and the SVR-LSM sensitivity map, respectively. Major significant clusters found by SVR-LSM confirmed and extended our previous findings with 2–sample t-test-based VLSM. In addition, SVR-LSM identified a cluster in the mid-to-anterior part of the left middle temporal gyrus and another in the left lateral prefrontal cortex [12,19]. The former area is strongly linked to verbal semantic processing [20], the latter to executive control of semantic retrieval [21]. The explanation could be that lesions in these areas cause semantic errors for different reasons. Regardless, it can be inferred from the present findings that these temporo-frontal areas form a deficit-contributing network for SE. This is because unlike VLSM, the multivariate SVR-LSM method picks up the coherence (correlation) of the different areas, as well as their independent contributions. By contrast, VSLSM only revealed brain-SE associations in left lateral prefrontal cortex (Fig. 3c).

The demonstrated superior performance of SVR-LSM against VLSM proved our hypothesis about the LSM sensitivity after incorporating the multivariate regression process. Different from the linear multiple regression, SVR-LSM has a nonlinear process during model training. Because of the various between-voxel interactive terms involved in the nonlinear process, SVR-LSM intrinsically takes correlations between voxels into account and subsequently improved brain-behavior relation detection sensitivity.

V. Conclusion

We fully evaluated a SVR-based multivariate lesion symptom mapping method. It is the first of its kind in the literature for mapping the brain-behavior relationship using lesion data. Evaluations using both synthetic data and real data showed the superior performance of the proposed SVR-LSM for LSM. While we only focused on LSM, the method can be used for predicting the continuous behavior score and extending it for neuroimaging data should be straightforward.

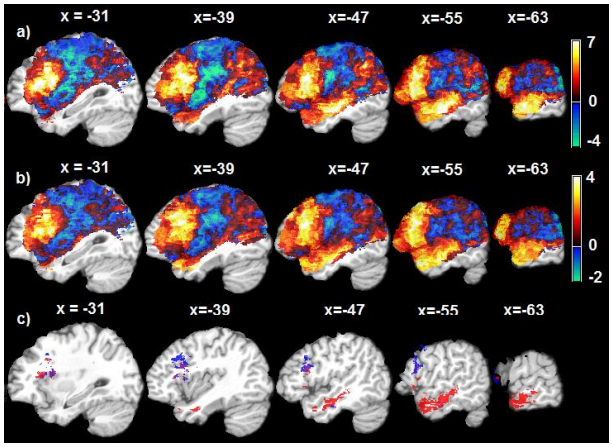

Fig. 3. Lesion-SE localizing results with SVR-LSM and VLSM methods, both methods include dTLVC to control the effect of total lesion volume. a) The non-thresholded SVR-LSM sensitivity map; b) the non-thresholded VLSM t-map; c) thresholded ($p \leq 0.001$, cluster size>50) permutation results with SVR-LSM (red) and VLSM (blue) method.

References

[1] Bates E. "Voxel-based lesion-symptom mapping." Nature Neuroscience, 6: 448-450, 2003.

[2] Rorden, C., & Karnath, H. O.. "Using human brain lesions to infer function: A relic from a past era in the fMRI age?" Nature Reviews. Neuroscience, 5(10): 813-819, 2004.

[3] Kimberg D.Y., Coslett H.B., Schwartz M.F.. "Power in voxel-based lesion-symptom mapping." J Cogn Neurosci, 19: 1067-80, 2007.

[4] Wang, Z., Faseyitan, O.K., Kimberg, D.Y., Coslett, H.B., Schwartz, M.F.. "Lesion-based Language Deficit Localization and Prediction Using Partial Least Square (PLS) Analysis," Annual Meeting of the Organization for Human Brain Mapping (OHBM), Beijing, China, Jun. 11, 2012.

[5] Smith,D.V., Clithero, J.A., Rorden, C., and Karnath, H.-O.. "Decoding the anatomical network of spatial attention." PNAS, 110(4):1518-1523, 2013.

[6] Kummerer D., Hartwigsen G., Kellmeyer P., Glauche V., Mader I., Kloppel S., et al.. "Damage to ventral and dorsal language pathways in acute aphasia". Brain, 136: 619–629, 2013.

[7] Zhang, Y., Kimberg, D.Y., Coslett H.B., Schwartz, M.F., Wang, Z. (2012). `` Language Deficit Prediction Using Brain Lesion Geometry Feature-based Support Vector Regression.'' Annual Meeting of the Organization for Human Brain Mapping (OHBM), Beijing, China, Jun. 11.

[8] Vapnik, V. N. . "The nature of statistical learning theory." Springer, 1995.

[9] Cortes, C. and Vapnik, V.. "Support-vector network." Machine Learning, 20:273–297, 1995.

[10] Wang Z.. "A hybrid SVM-GLM approach for fMRI data analysis," NeuroImage, 46(3):608-615, 2009.

[11] Smola A. J. and Schölkopf B.. "A Tutorial on Support Vector Regression." Statistics and Computing, 14(3):199-222, 2004.

[12] Schwartz M.F., Kimberg D.Y., Walker G.M., Faseyitan O., Brecher A., Dell G.S.. "Anterior temporal involvement in semantic word retrieval: VLSM evidence from aphasia." Brain. 132: 3411-3427, 2009.

[13] Walker, G.M., Schwartz, M.F., Kimberg, D.Y., Faseyitan, O., Brecher, A., Dell, G.S., et al.. "Support for anterior temporal involvement in semantic error production in aphasia: new evidence from VLSM." Brain Lang, 117: 110–22, 2011.

[14] Rasmussen, P.M., Madsen K.H., Lund T.E., Hansen L.K.. "Visualization of nonlinear kernel models in neuroimaging by sensitivity maps." NeuroImages, 55: 1120-1131, 2011.

[15] Chang C. C. and Lin C. J.. "LIBSVM : a library for support vector machines." ACM Transactions on Intelligent Systems and Technology, 2:27:1--27:27, 2011.

[16] Philadelphia Naming Test, available online: http://www.mrri.org/philadelphia-naming-test

[17] Schwartz, M. F., Brecher, A., Whyte, J. W., & Klein, M. G.. A patient registry for cognitive rehabilitation research: A strategy for balancing patients' privacy rights with researchers' need for access. Archives of Physical Medicine and Rehabilitation, 86(9), 1807-1814, 2005.

[18] Metz C.E., "Basic principles of ROC analysis", Semin Nucl Med, 8(4):283-298, 1978.

[19] Schwartz M.F., Faseyitan O., Kim J. and Coslett, H. B.. "The dorsal stream contribution to phonological retrieval in object naming." Brain 135: 3799-3814, 2012.

[20] Mesulam, M, Wieneke, C, Hurley, R, Rademaker, A, Thompson, CK, Weintraub, S & Rogalski, EJ, "Words and objects at the tip of the left temporal lobe in primary progressive aphasia", Brain, vol. 136, pp. 601-18, 2013.

[21] Schnur, TT, Schwartz, MF, Kimberg, DY, Hirshorn, E, Coslett, HB & Thompson-Schill, SL, "Localizing interference during naming: Convergent neuroimaging and neuropsychological evidence for the function of Broca's area", Proceedings of the National Academy of Sciences, vol. 106, no. 1, pp. 322-7, 2009.